Properties of magnetically diluted nanocrystals prepared by mechanochemical route

P. Baláž [a,*], I. Škorvánek [b], M. Fabián [a], J. Kováč [b], F. Steinbach [c], A. Feldhoff [c], V. Šepelák [a], J. Jiang [d], A. Šatka [e], J. Kováč [e]

[a] Institute of Geotechnics, Slovak Academy of Sciences, 043 53 Košice, Slovakia
[b] Institute of Experimental Physics, Slovak Academy of Sciences, 043 57 Košice, Slovakia
[c] Leibnitz University of Hannover, Institute of Physical Chemistry and Electrochemistry, 301 67 Hannover, Germany
[d] International Center for New-Structured Materials, Zhejiang University, 310 027 Hangzhou, China
[e] Slovak University of Technology and International Laser Centre, 812 19 Bratislava, Slovakia

ARTICLE INFO

ABSTRACT

The bulk and surface properties of magnetically diluted $Cd_{0.6}Mn_{0.4}S$ nanocrystals synthesized by solid state route in a planetary mill were studied. XRD, SEM, TEM (HRTEM), low-temperature N_2 sorption, nanoparticle size distribution as well as SQUID magnetometry methods have been applied. The measurements identified the aggregates of small nanocrystals, 5–10 nm in size. The homogeneity of produced particles with well developed specific surface area ($15–66\,m^2\,g^{-1}$) was documented. The transition from the paramagnetic to the spin-glass-like phase has been observed below ∼40 K. The changes in the magnetic behaviour at low temperatures seem to be correlated with the formation of the new surface area as a consequence of milling. The magnetically diluted $Cd_{0.6}Mn_{0.4}S$ nanocrystals are obtained in the simple synthesis step, making the process attractive for industrial applications.

1. Introduction

In recent years, semiconductor nanocrystals (QD) have attracted much attention due to their great potential for technology [1]. Optical, electrical, magnetic and other properties of QD with respect to corresponding bulk materials are modified considerably, offering a number of potential applications. The introduction of magnetic ions in semiconductor nanocrystals results in new materials called dilute magnetic semiconductors (DMS) [2–4]. Here combination of two most application based properties, namely semiconducting and magnetic is created [5]. Among possible magnetic dopants (e.g. Fe, Co, Mn) manganese based II–IV DMS have attracted considerable attention as a result of the large exchange interaction between the band electrons and Mn^{2+}. An important example of the Mn^{2+} doped II–IV semiconductors family is $Cd_{1-x}Mn_xS$ system [6]. There are several methods to prepare DMS like spray pyrolysis, electrodeposition, vacuum evaporation, screen printing, photochemical deposition, chemical bathdeposition and sputtering [1,7,8].

Mechanochemical synthesis belongs to the non-equilibrium routes which are currently used to prepare nanocrystalline powders [9]. In this procedure a high-energy mill is applied as a mechanochemical reactor where nanostructures can be obtained in the simple, one pot solid state synthesis step. Thus mechanochemical synthesis is a very straightforward, one-step, ambient temperature process that can be utilized to make magnetically diluted $Cd_{1-x}Mn_xS$ nanocrystals. The application of mechanochemistry leads to production of a high density of crystal defects in the synthesized nanostructures [10–13]. The products are well homogenized with particles in nanorange and possessing extraordinary properties.

In this paper, we report the mechanochemical solid state synthesis and characterization of magnetically diluted $Cd_{0.6}Mn_{0.4}S$ nanocrystals.

2. Experimental

Mechanochemical solid state synthesis of $Cd_{1-x}Mn_xS$ ($x = 0.4$) nanocrystals was performed in a laboratory planetary mill Pulverisette 6 (Fritsch, Germany). The following milling conditions were used: loading of the mill with 50 balls (tungsten carbide) of 10 mm diameter; rotation speed of the planet carrier: 500 rpm, milling time: 5, 10 and 20 min, working atmosphere: argon. $Cd_{0.6}Mn_{0.4}S$ nanocrystals were synthesized from the corresponding acetates $(CH_3COO)_2Cd\cdot2H_2O$, $(CH_3COO)_2Mn\cdot4H_2O$ and sodium sulphide $Na_2S\cdot9H_2O$ (Ites, Slovakia) according to the equation

$$0.6\,(CH_3COO)_2Cd\cdot2H_2O + 0.4\,(CH_3COO)_2Mn\cdot4H_2O + Na_2S\cdot9H_2O$$
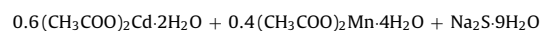
$$\rightarrow Cd_{0.6}Mn_{0.4}S + 2\,CH_3COONa + 11.8\,H_2O \qquad (1)$$

* Corresponding author. Tel.: +421 055 7922603; fax: +421 055 7922604.
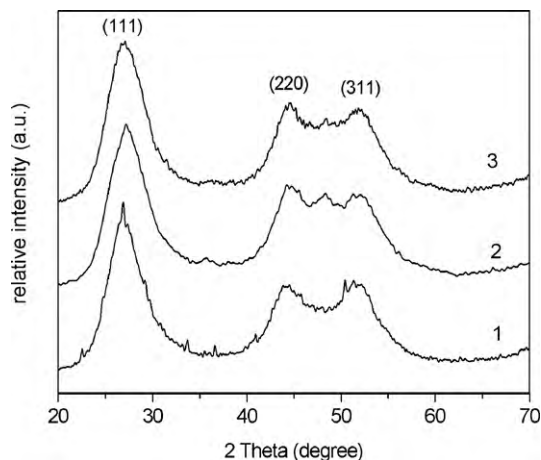E-mail address: balaz@saske.sk (P. Baláž).

Fig. 1. XRD patterns of the synthesized $Cd_{0.6}Mn_{0.4}S$ nanocrystals: (1) chemically precipitated, (2) milled 5 min, (3) milled 20 min.

After completion of reaction (1) the produced nanocrystals have been washed, decanted and dried according to the procedure described in [11]. The properties of mechanically synthesized $Cd_{1-x}Mn_xS$ nanocrystals were compared with those prepared by precipitation from aqueous solutions of $(CH_3COO)_2Cd·2H_2O$ and $(CH_3COO)_2Mn·4H_2O$, respectively. The specific surface area was determined by the low-temperature nitrogen adsorption method in a Gemini 2360 sorption apparatus (Micromeritics, USA). The dispersion and the particle size analysis of samples were measured on Nanophox particle sizer (Sympatec, Germany) using the photon cross correlation spectroscopy method. The equipment works with the build-up He–Ne laser diode with the maximum output 10 mW and the wavelength of radiation $\lambda = 0.6328 \,\mu m$. The samples were taken directly from the mill and after ultrasonification the images of fine particles present in the liquid state were taken. The measured results have been processed using Window 5 software. The XRD measurements were performed by employing the X-ray difractometer Philips PW 1820. The CuKα radiation ($\lambda = 1.5406 \,Å$) was used. The counting time was 2 s per step and the step size was 0.05°. The synthesized samples were also analysed using FE–SEM LEO 1550 scanning microscope. The samples were left uncovered from any conductive material in order to keep their original properties. The HRTEM images of as-milled $Cd_{0.6}Mn_{0.4}S$ nanocrystals were obtained from a FE–TEM JEOL JEM–2100 F transmission electron microscopy. The measurements of magnetization as a function of temperature and applied field have been performed by a commercial SQUID magnetometer in temperature range from 2 K to 300 K. We have used the Magnetic Property Measuring System model MPMS-XL-5 (Quantum Design, USA) equipped with 5 T superconducting magnet.

3. Results and discussion

Fig. 1 shows the powder XRD patterns of $Cd_{0.6}Mn_{0.4}S$ nanocrystals as a function of the synthesis procedure and/or milling
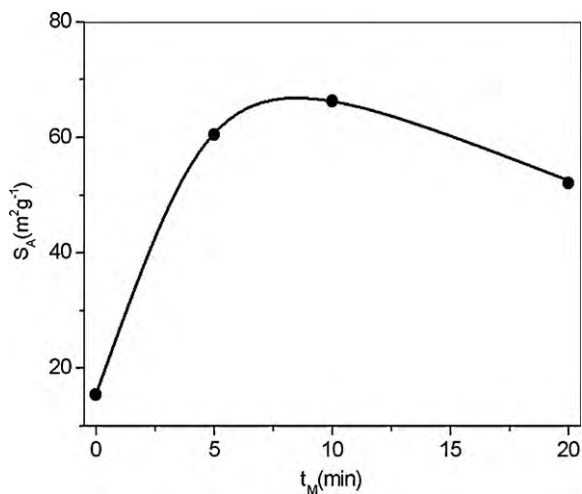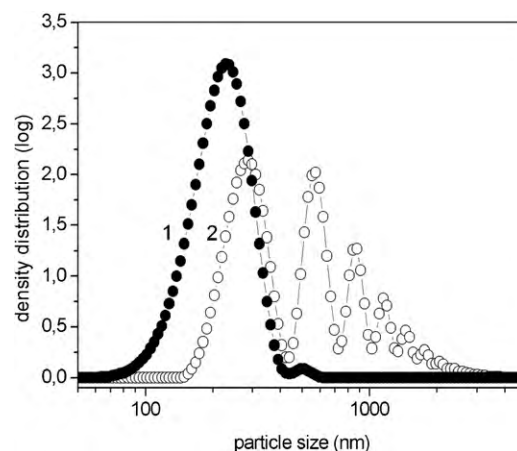

Fig. 3. Particle size distribution for $Cd_{0.6}Mn_{0.4}S$ nanocrystals: (1) chemically precipitated, (2) milled 20 min.

time. All peaks in the XRD patterns indicate broadening which is characteristic for the nanoparticles. The patterns of $Cd_{0.6}Mn_{0.4}S$ for chemically precipitated sample (1) and mechanochemically synthesized (2 and 3) are practically identical. The patterns can be indexed as hawleyite-phase structure (JCPDS 10–454) with strongly characteristic (1 1 1), (2 2 0) and (3 1 1) reflections. The cubic phase with (1 1 1), (2 2 0) and (3 1 1) planes has been also identified in $Cd_{1-x}Mn_xS$ ($x = 0$–0.15) films prepared by spray pyrolysis technique [5] as well as in our previous paper on the mechanochemically synthesized $Cd_xZn_{1-x}S$ nanocrystals ($x = 0$–1) where gradual transformation from sphalerite to hawleyite as a consequence of milling has been observed [12].

The dependence of the new surface area formation on milling time in $Cd_{0.6}Mn_{0.4}S$ is given in Fig. 2. The value $S_A = 15.5 \, m^2 \, g^{-1}$ has been obtained for chemically precipitated (non-milled) sample. The milled samples are manifested with higher values. From the plotted data one can conclude that the highest value of $S_A = 66.3 \, m^2 \, g^{-1}$ is at milling time 10 min. At shorter milling period the increase in S_A values is dominating with the value $S_A = 60.5 \, m^2 \, g^{-1}$ for sample synthesized at milling time 5 min. Longer time of milling causes agglomeration of as-prepared nanoparticles and after 10 min of mechanochemical treatment the decrease in the S_A values can be noticed. In general, the mechanochemically prepared $Cd_{0.6}Mn_{0.4}S$ nanocrystals have 3–4 times higher specific surface area in com-
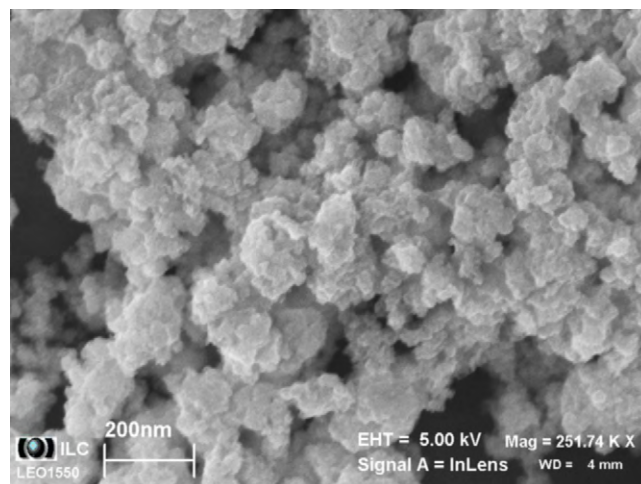

Fig. 2. Specific surface area, S_A vs. milling time, t_M for $Cd_{0.6}Mn_{0.4}S$ nanocrystals.

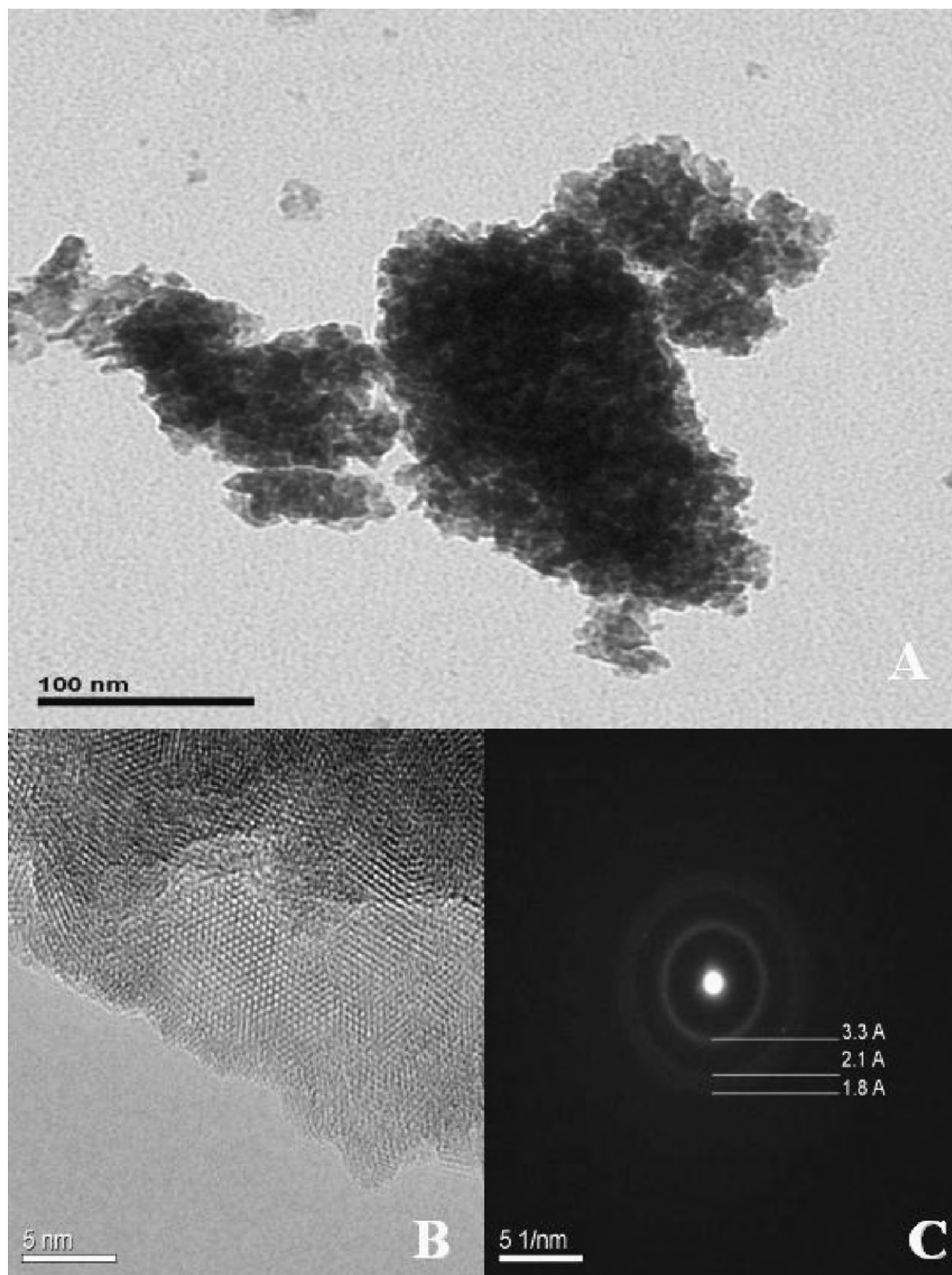**Fig. 4.** FE-SEM of mechanochemically synthesized $Cd_{0.6}Mn_{0.4}S$ nanocrystals, milling 10 min.

Fig. 5. TEM (A), HRTEM (B) and SAED (C) patterns of mechanochemically synthesized $Cd_{0.6}Mn_{0.4}S$ nanocrystals, milling 10 min.

parison with the chemically precipitated sample which can be attributed to the polydisperse distribution of particles. This fact is an ultimate challenge for application of semiconductor nanocrystal particles in technology of modern materials application where

a developed surface is needed, e.g. in heterogenous catalysis. It is worth to mention that such particles have been obtained by solid state synthesis technique where reactants into milling have been applied as solids. In comparison, the liquid solutions were used

by precipitation technique. Exclusion of excess solution is another advantage of the solid state approach.

The dispersion and the particle size of $Cd_{0.6}Mn_{0.4}S$ nanoparticles were characterized by photon cross correlation spectroscopy as shown in Fig. 3. The plot for chemically precipitated sample (1) indicates well isolated nanoparticles with the average hydrodynamic parameter $d = 240$ nm. However, in milled $Cd_{0.6}Mn_{0.4}S$ particles (2) several individual peaks are visible. The largest one belongs to the average hydrodynamic diameter of particles $d = 298$ nm. In spite of the higher specific surface area ($55.1\ m^2\ g^{-1}$ in comparison with $15.5\ m^2\ g^{-1}$ for chemically precipitated sample), there is a broader distribution spectrum of the milled samples overlapping micrometer dimensions.

The morphology of particles as well as their internal structure can be documented by SEM and TEM studies. FE–SEM micrograph of mechanochemically synthesized $Cd_{0.6}Mn_{0.4}S$ nanoparticles is given in Fig. 4.

There is a strong tendency for cluster formation by milling where individual nanoparticles form aggregates during mechanosynthesis. The larger aggregates, less than 200 nm in size are formed by the smaller entities where particle size is approx. 30 nm. After careful inspection the smaller particles can be also identified. TEM, HRTEM and SAED study of the milled sample is given in Fig. 5. The previous formation given by SEM pattern is further refined. TEM bright-field micrographs show nanocrystals consisting of crystallites mostly in the 5–10 nm size range. The atomic planes on HRTEM pattern are clearly demonstrated. Fig. 5(B) shows a well defined cluster of ∼7 nm with a hexagonal profile. The polycrystalline character of the nanocrystals can be seen from the Debye–Scherrer rings on SAED pattern. The rings are widened and dispersed which is a consequence of the presence of very small particles. The absence of dot doped in the rings can be attributed to the non-uniform distribution of Mn^{2+} cations in the structure as well as core–shell structure of as-prepared material.

Fig. 6 shows the results of the field-cooled (FC), zero-field-cooled (ZFC) dc-magnetization measurements for chemically precipitated and mechanochemically synthesized nanocrystals. The sequence of these measurements was as follows: (i) the samples were first cooled from 60 K to 2 K at zero-field, and after application of 100 Oe the ZFC magnetization was determined during warming to 60 K, (ii) the FC curves were recorded during the cooling from 60 K down to 2 K in an external field of 100 Oe.

The obtained ZFC-FC dependences resemble the features that are characteristic for transition from the paramagnetic to the spin-glass-like phase, where the magnetic moments are frozen in
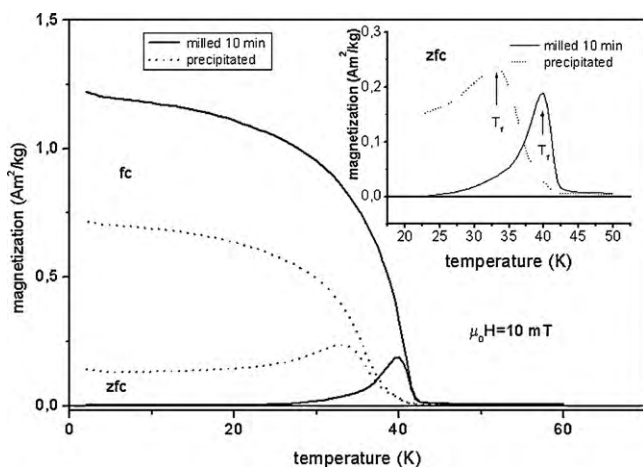

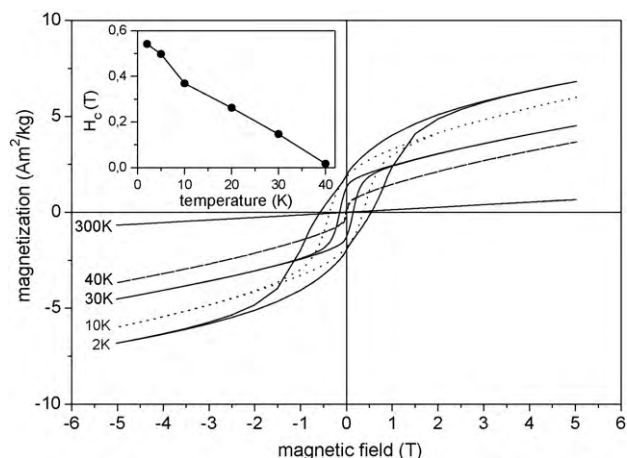**Fig. 7.** Hysteresis loops of mechanochemically synthesized $Cd_{0.6}Mn_{0.4}S$ nanocrystals (milling 10 min) taken at indicated temperatures. The inset shows a temperature dependence of the coercive field

random directions due to competing exchange interactions. Indeed, such transition has been reported for the $Cd_{1-x}Mn_xS$ diluted magnetic semiconductors with compositions from $x = 0.3$–0.5 in the form of both "bulk" materials [14] as well as chemically synthesized ultrafine particles [15]. The appearance of a well defined cusp in the ZFC magnetization curves is associated with the freezing temperature, T_f, below which a disordered spin-glass phase exists. The position of cusp increases from ∼33 K for the chemically precipitated sample to 39.8 K for the sample synthesized at milling time 10 min.

The observed strong irreversibility between ZFC and FC magnetization curves seems to be related to the difference between the random distribution of the frozen magnetic moments after zero-field cooling and the ordered state which can be obtained after the cooling the system in an applied field. In ZFC regime the external field has to overcome an array of the random local anisotropy axes, before the various magnetic moments can point along the field direction. Clearly, the increase of temperature toward T_f will facilitate this process due to the thermally assisted jumps of the moments away from their anisotropy-pinned "frozen" orientation. The increase of T_f after milling seems to be correlated with the formation of new surface areas that are associated with a higher degree of lattice and/or spin disorder and related frustration effects.

Magnetic properties of the sample synthesized at milling time 10 min were investigated by measuring of hysteresis loops versus temperature. In Fig. 7, the magnetic hardening at low temperatures is evidenced by the increase of coercive field. As shown by the inset of Fig. 7, upon lowering the temperature from 40 K to 2 K, the coercive field increases from 0.016 T to 0.54 T. The loop taken at 300 K shows typical paramagnetic behaviour, i.e. no ferromagnetic response at room temperature could be detected as it was reported recently for $Cd_{0.6}Mn_{0.4}S$ nanoclusters [16]. The value of coercive field at 2 K for the sample synthesized at milling time 10 min is about fivefold larger than the coercive field of chemically precipitated sample ($H_c \approx 0.12$ T) at this temperature. This increase is believed to be again correlated with the formation of new surface areas with a higher density of lattice defects upon milling characterized by enhanced surface anisotropy.

4. Conclusions

In this paper the one-step mechanochemical solid state synthesis of diluted magnetic $Cd_{0.6}Mn_{0.4}S$ nanocrystals differing by

Fig. 6. ZFC and FC magnetization versus temperature for chemically precipitated and milled (10 min) $Cd_{0.6}Mn_{0.4}S$ nanocrystals.

surface and bulk properties has been demonstrated. The non-conventional one-step route to $Cd_{1-x}Mn_xS$ synthesis offers several advantages over traditional processing routes, including low-temperature solid state reactions and suitability the low cost, large-scale production of nanopowders. The nanocrystals with well developed surface areas ($15–66\,m^2\,g^{-1}$) and in nanosizedimensions ($5–10\,nm$) were obtained. The mechanochemical synthesis which was applied has considerable possibility for easily scaling up the production of nanocrystals under ambient conditions in reasonable time without the applications of any liquid in preparation step. The observed changes of magnetic properties point out the important role of the new surface areas formed during mechanochemical processing that are associated with a higher degree of lattice and/or spin disorder.

Acknowledgements

References

[1] A. Rogach (Ed.), Semiconductor Nanocrystalline Quantum Dots, Heidelberg, Berlin, 2008.
[2] J.K. Furdyna, J. Kossut, Semiconductors and Semimetals, Vol. 25, Academic Press, New York, 1988.
[3] M.P. Pileni, Catalysis Today 58 (2000) 151.
[4] M.P. Pileni, in: K.J. Klabunde (Ed.), Nanoscale Materials in Chemistry, John Wiley & Sons, Inc., New York, 2001, p. 61.
[5] N. Badera, B. Godbole, S.B. Srivastava, P.N. Vishwakarma, L.S. Sharath Chandra, D. Jain, V.G. Sathe, V. Ganesan, Solar Energy Materials and Solar Cells 92 (2008) 1646.
[6] P. Sudgahar, R. Sathyamoorthy, S. Chandramohan, S. Senthilarasu, S.H. Lee, Materials Letters 62 (2008) 2430.
[7] L. Levy, D. Ingert, N. Feltin, M.P. Pileni, Journal of Crystal Growth 184/185 (1990) 337.
[8] F. Iaconi, I. Salaouru, N. Apetroei, A. Vasile, C.M. Teodorescu, D. Macovei, Journal of Optoelectronics and Advanced Materials 8 (2006) 266.
[9] P. Baláž, Mechanochemistry in Nanoscience and Minerals Engineering, Springer, Berlin Heidelberg, 2008.
[10] P. Baláž, Extractive Metallurgy of Activated Minerals, Elsevier, Amsterdam, 2000.
[11] P. Baláž, E. Boldižárová, E. Godočíková, J. Briančin, Materials Letters 57 (2003) 1585.
[12] E. Dutková, P. Baláž, P. Pourghahramani, V. Anh, Nguyen, V. Šepelák, A. Feldhoff, J. Kováč, A. Šatka, Solid State Ionics 179 (2008) 1242.
[13] E. Dutková, P. Baláž, P. Pourghahramani, S. Velumani, J.A. Ascencis, N.G. Kostova, Journal of Nanoscience and Nanotechnology 9 (2009) 1.
[14] Y.Q. Yang, P.H. Keesom, J.K. Furdyna, W. Giriat, Journal of Solid State Chemistry 49 (1983) 20.
[15] R.J. Bandaranayake, J.Y. Lin, H.X. Jiang, C.M. Sorensen, Journal of Magnetism and Magnetic Materials 169 (1997) 289.
[16] P. Sudhagar, R. Sathyamoorthy, S. Chandramohan, S. Senhilarasu, S.H. Lee, Materials Letters 62 (2008) 2430.